

# At what data length do cerebral autoregulation measures stabilise?

Adam Mahdi<sup>1</sup>, Dragana Nikolic<sup>2</sup>, Anthony A. Birch<sup>3</sup>, Stephen J. Payne<sup>1</sup>

<sup>1</sup>*Department of Engineering Science, University of Oxford, UK.*

<sup>2</sup>*Institute of Sound and Vibration Research, University of Southampton, UK.*

<sup>3</sup>*Department of Medical Physics and Bioengineering, Southampton General Hospital, UK.*

## Abstract

Cerebral autoregulation is commonly assessed through mathematical models that use non-invasive measurements of arterial blood pressure and cerebral blood flow velocity. There is no agreement in the literature as to what is the minimum length of data needed for the cerebral autoregulation coefficients to stabilise. We introduce a simple empirical tool for studying the minimum length of time series needed to parameterise three popular cerebral autoregulation coefficients ARI, Mx and Phase (in the low frequency range [0.07-0.2] Hz), which can be easily applied in a more general context. We use our recently collected data, from which we select high quality (absence of non-physiological artefacts), baseline ABP-CBFV time series (16-minute each). The data were beat-to-beat averaged and downsampled at 10 Hz. On average, ARI exhibits greater variability than Mx and Phase, when calculated for short intervals; however, it stabilises fastest. Our results show that values of ARI, Mx and Phase calculated on intervals shorter than 3 min (1800 samples), 6 min (3600 samples) and 5 min (3000 samples), respectively, may be very sensitive to changes in the length of data interval.

**Keywords:** cerebral autoregulation, blood pressure, cerebral blood flow, data length

## 1 Introduction

Cerebral autoregulation (CA) is a term that encompasses many different control mechanisms responsible for maintaining cerebral blood flow at an appropriate, approximately constant, level despite changes in arterial blood pressure (ABP). Poor CA has been linked with several clinical disorders such as stroke [1], subarachnoid haemorrhage [2], head injury [3], syncope and cerebral microvascular diseases. Therefore, it is of great interest to have fast, reliable and non-invasive autoregulation assessment methods.

Typically, CA is assessed through different mathematical models [4]–[6] that use non-invasive measurements of ABP and cerebral blood flow velocity (CBFV) and produce a metric (e.g. a numerical value) from a certain interpretable range. Unfortunately, despite a large body of literature, a gold standard approach is not available. A lack of standardized methods is likely to be a significant contributor.

It is surprising that the questions as to what is the least amount of data needed to calibrate models and to obtain physiologically significant assessment of CA have been given little attention, with the exception of [7]. One possible reason for this gap in the literature is that these types of studies typically require long (>10 min) and high quality (lack of non-physiological artefacts) time series data. Also, to limit the effects of potential confounders, carefully designed data collection protocols are needed, but they are difficult to implement.

In the current paper we study the minimum data length needed to parameterise three popular CA measures: the autoregulation index (ARI), the correlation coefficient  $M_x$  and the phase shift between ABP and CBFV calculated at low frequency range. We introduce a simple empirical tool, the *expanding window sensitivity*, designed to monitor the fluctuations of the CA measures as we expand the data window. Together with the concept of the *corridor of stability*, i.e. the size of fluctuations we agree to tolerate (previously used in [8]) we can identify the *point of stability* for each measure under consideration (see Section 2.5).

## 2 Methods

### 2.1 Data collection

With approval from an NHS ethics committee (14/NI/1146) 10 young volunteers ( $23.5 \pm 3.0$  years,  $172.1 \pm 12.5$  cm,  $66.6 \pm 19.0$  kg, BMI  $22.1 \pm 4.2$ , SBP  $124.0 \pm 15.0$  mmHg, DBP  $72.0 \pm 5.0$  mmHg, 3 female) and with no history of vascular disease were recruited. All volunteers attended for cerebral autoregulation studies on 5 separate occasions within a one-week period. Data used for this analysis has been selected from one of those 5 visits for each subject.

Volunteers were asked to lie in the supine position on a comfortable bed, with a head supported on a pillow, for the whole duration of data collection. Both middle cerebral artery velocities were monitored with transcranial Doppler ultrasound (Dopplerbox, DWL, GmbH, Singen, Germany) and ABP was monitored using a Finometer (Finapres Medical Systems, Amsterdam, The Netherlands). Three lead ECG was also applied and recorded (ECG100C BIOPAC Systems Inc, Goleta, CA USA). The arterial blood pressure (ABP), the left and right cerebral flow velocity (CBFV-L and CBFV-R respectively) and ECG signals were simultaneously recorded over approximately 18 minutes of rest. The signals were sampled at 125 Hz (with an exception of the ECG signal which was sampled at 250 Hz) and stored for offline analysis using a data acquisition system (MP150, BIOPAC Systems Inc, Goleta, CA USA). Following instrumentation, which would typically take 10 to 15 minutes, volunteers were asked to stay quiet and still, without falling asleep, while data were recorded. Background noise was kept to a minimum.

### 2.2 Data preprocessing

The raw signals were low-pass filtered using a fourth-order Butterworth filter with a cut-off frequency of 20 Hz applied in the forward and backward direction to compensate for phase shifts. Isolated spikes in the CBFV signals were removed using the median filter of the 9th order and the most prominent remaining ones were removed by linear interpolation. The beat-to-beat average (mean) values of the ABP, CBFV-L and CBFV-R were then computed for each cardiac cycle using the R-peaks detected from the ECG signal. In order to create a time series with a uniform time base, the mean signals were interpolated using a third-order polynomial and resampled at 10 Hz.

### 2.3 Cerebral autoregulation indices

*ARI*. Tiecks et al. [9] proposed a set of difference equations to predict CBFV as a response to a change in ABP, from which an autoregulation index (ARI) is calculated. The method itself and its variations have been used extensively to provide a quantitative assessment of CA [38, 32, 2]. The index ranges from 0 (the absence of autoregulation) to 9 (the best autoregulation). For more details, related to the computational aspects of ARI, see the Appendix.

*$M_x$* . The  $M_x$  index was computed here as Pearson's correlation coefficient between the mean ABP and mean CBFV over a certain interval [3]. If a moving window is applied the values were averaged

for each window size and each patient. Some authors [10] have suggested that the values less than 0.3 indicate an intact CA, while values above 0.3 indicate failure of autoregulation.

*Phase.* The phase of the transfer function have been widely applied to assess cerebral autoregulation [11]-[13]. In this study, it was computed as follows. First, the mean ABP and CBFV signals were further downsampled to 1 Hz, normalized by their mean values and detrended representing the signal change in %. The ARX model of order (2,3) was estimated in the least-square sense using the normalised and detrended mean ABP and CBFV. Autoregulation was assessed by the mean phase (i.e. average values of the phase) of the estimated transfer response calculated in the low frequency range [0.07-0.2] Hz.

## 2.4 Expanding window sensitivity

We introduce a simple measure designed to quantify how sensitive a CA measure is with respect to changes in the length of the time series used for its calculation. This, in turn, will be used to assess how much data are needed for a stable parameterisation of a given CA model.

We denote by  $P_t$  and  $V_t$  the ABP and CBFV time series defined on some time interval  $t = [t_0, t_1]$ . With this notation we denote both time series by  $d_j = (P_{t_j}, V_{t_j})$ , where  $t_j = [t_0, t_0 + j\Delta t]$ . Note that  $j\Delta t$  is the length of the expanding window for each increment  $j$ , where  $j = 1, \dots, N$ , and  $N$  is the maximum number of intervals  $\Delta t$  in the recording. Let  $c(d_j)$  be a CA measure of interest (e.g. ARI, Mx or Phase), calculated using time series  $d_j$ . The *expanding window sensitivity* at  $d_j$  is computed (for each subject) as

$$\mathbb{E}(d_j) = |c(d_{j+1}) - c(d_j)| \quad \text{for } j = 1, \dots, N - 1. \quad (1)$$

We report the mean and standard deviation of expanding window sensitivity,  $\mathbb{E}(d_j) \pm SD$ , calculated across all subjects.

## 2.5 Corridor and point of stability

The mean expanding window sensitivity  $\mathbb{E}(d_j)$  can be interpreted as the average fluctuation of a CA measure  $c(d_j)$  calculated using  $d_j$ . We note that the smaller  $\mathbb{E}(d_j)$  the more stable  $c(d_j)$ . To make the discussion of stability more precise, we introduce the concept of the *corridor of stability*, that is the corridor around zero where the deviations of  $\mathbb{E}(d_j)$  are tolerated, see [8]. The corridor of stability is characterized by its width, which depends on a specific problem (e.g. a scale the model operates on).

Typically, as the sample size increases, the values of  $\mathbb{E}(d_j)$  get (stochastically) smaller until they stabilise. We define the *point of stability* as the minimal data length (or sample size) such that  $\mathbb{E}(d_j)$  stays within the selected corridor of stability.

## 2.6 Moving window variability

Here we introduce a method designed to quantify the variability associated with a CA estimates irrespectively of the fixed beginning of the data intervals used for their computation. We consider a CA measure  $c(d_m)$ ,  $d_m = (P_{t_m}, V_{t_m})$ , on the moving window  $t_m = [(m-1)s\Delta t, ms\Delta t]$ ,  $m = 1, \dots, N_s$ , where  $N_s$  is the total number of non-overlapping windows of size  $w_s$  in the recording. The index  $m$  represents the position of the window  $t_m$  of size  $w_s = s\Delta t$  that moves along the recording. We define *moving window variability* as standard deviation of the CA measures,  $c(d_m)$ , calculated on each moving window:

$$M(w_s) = \text{std}(c(d_1), \dots, c(d_{N_s})). \quad (2)$$

We report the mean moving window sensitivity  $\mathbb{M}(w_s) \pm SD$  calculated across all subjects.

### 3 Results

*Data characteristics.* Table 1 gives the mean, standard deviation and coefficient of variability (CoV) of the mean ABP, mean CBFV, end-tidal  $\text{CO}_2$  ( $\text{etCO}_2$ ) and heart rate (HR) for the whole dataset. The ‘Mean’ and ‘SD’ refer to the mean and standard deviation of the values calculated for each subject along time.

*Expanding window sensitivity.* Figure 1 (left column) show the trajectories of ARI, Mx and Phase calculated for the step increment  $\Delta t = 30\text{s}$  of the ABP-CBFV time series data over the whole 16-minute interval for all 10 individuals. Here, the beginning of each expanding window is set to  $t_0 = 0$ . Figure 1 (right column) show the mean (red line) and standard deviation (vertical bars) of the expanding window sensitivity,  $\mathbb{E}(d_j) \pm SD$ , calculated across all subjects. The dotted lines (left column) indicate the point of stability corresponding to the corridor of stability (grey area, right column). We note that the fluctuations of ARI, Mx and Phase reduce as more data are used for model calibration.

*Moving window variability.* Figure 2 (top five rows) show ARI, Mx and Phase values calculated for the indicated window size as it moves along the 16-minute long recording. Figure 2 (bottom row) show the moving window variability  $\mathbb{M}(w_s)$  for the window size  $w_s = s\Delta t$ , where  $s = 1, \dots, 5$  and  $\Delta t = 30\text{s}$ . The values of  $\mathbb{M}(w_s)$  decrease as the moving window gets wider.

### 4 Discussion

There is no consensus in the literature regarding what is the appropriate amount of data (typically ABP and CBFV) needed to parametrise CA models. A variety of data lengths have been used (see e.g. [10], [14], [15], [16]). Long data recordings are typically divided into 1-5 minute intervals, for which Mx is computed and results are averaged for the whole measurement period. On the other hand, model-based approaches, including ARI, have been calibrated using shorter time series including 2 min [17], 5 min [18] and 10 min [19] intervals.

We introduced here two simple methods, the expanding window sensitivity (Section 2.5) and moving window variability (Section 2.6), to study the effects of data length on CA indices. They are based on the assumption that the underlying overall physiological mechanisms involved in maintaining autoregulation are approximately constant in the considered interval.

The expanding window sensitivity together with the corridor of stability allows us to empirically determine (for the given dataset) the interval needed for model calibration. The mean values of the expanding window sensitivity decrease (see Figure 1: right column, red line) as indices reach a plateau. By setting the corridor of stability around the plateau we identified the point of stability, i.e. the minimal data length, for which the mean sensitivity stays within this corridor.

Our discussion is contingent upon the specific dataset available and the type of preprocessing we have used. We note that here the raw signals were beat-to-beat averaged and resampled at 10 Hz, which is a common practice in the context of autoregulation. The discussion of other sampling frequencies and their effects on the results is beyond the scope of this paper.

Our results show that the CA indices fluctuate significantly for short intervals (see Figure 1: left column), which is reflected by the large values of the expanding window sensitivity (see Figure 1: right column). Also, ARI exhibits larger variability than Mx when calculated on shorter intervals but unlike Mx, its values stabilise quickly and exhibit smaller fluctuations for longer intervals. Although we are unable to make firm recommendation as what is the minimal length of ABP and CBFV time

series needed to estimate the indices, based on the results obtained here, we can say that ARI, Mx and Phase calculated on intervals shorter than 3, 6 and 5 minutes respectively, may not be reliable as they exhibit very large variability.

The size of fluctuations of the CA indices can be influenced by many factors including physiological artefacts (e.g. ectopic beats), non-physiological artefacts (e.g. square wave, saturation, impulse, signal loss) [20], [21] and outliers [22]. Although we made an effort to remove all the visible artefacts due to measurement error in instrumentation, the unexpected physiological anomalies that do not fit the pattern are much harder to account for [23]. The non-linear character of the underlying CA phenomena is potentially another important contributor to the high variability of the CA measures.

Figure 2 gives additional evidence that non-physiological artefacts may bias CA indices for short data segments. As we move along the signal, ARI, Mx and Phase vary significantly for smaller windows. However, this variability decreases as we consider longer windows, which is a general trend shown in Figure 2 (bottom row).

The study has several limitations. The approximation of cerebral blood flow by CBFV measured in the MCA is only valid if the diameter of the MCA is constant. The use of the Finapres monitor to provide continuous estimates of ABP is another potential source of error. The question whether the dispersion in CA estimates comes from the ‘noise’ or actual physiological variability is a difficult one. The common assumption is that the input signal is ‘clean’ and the output has independent added stationary (Gaussian) noise. Some recent studies have reported that the prediction of estimation errors based on that assumption accounts for much, but not all the intra-subject variability observed (even within the same recording) [24]. The actual problem is even more complex because the input signal is not clean (recording from Finapres), the linear model as well as model order we use is not perfect and noise is most likely not stationary or time-invariant. Furthermore, the ARI method followed the original paper by Tiecks et al. [9], however, alternative implementations have also been proposed. In particular, Panerai et al. [13] showed that a combination of time series modelling (ARMA) and the best fit to one of the ARI step responses is less susceptible to physiological sources of variability.

In conclusion, we introduced simple tools to study the minimal data length needed to stabilise three popular CA indices: Mx, ARI and Phase. However, the methods are applicable in the wider context. Our hope was to draw the attention of researchers to consider more carefully the effects of the data length on model calibration and CA estimates.

## Acknowledgement

The authors acknowledge the support of the EPSRC project EP/K036157/1. The authors would like to thank RB Panerai and DM Simpson for valuable comments during the preparation of this manuscript.

## References

- [1] S. L. Dawson, M. J. Blake, R. B. Panerai, and J. F. Potter, “Dynamic but not static cerebral autoregulation is impaired in acute ischaemic stroke,” *Cerebrovasc. Dis.*, vol. 10, no. 2, pp. 126–32, 2000.
- [2] C. A. Giller, “The frequency-dependent behavior of cerebral autoregulation,” *Neurosurgery*, vol. 27, no. 3, pp. 362–368, 1990.
- [3] M. Czosnyka, P. Smielewski, P. Kirkpatrick, D. K. Menon, and J. D. Pickard, “Monitoring of cerebral autoregulation in head-injured patients,” *Stroke*, vol. 27, no. 10, pp. 1829–1834, 1996.
- [4] S. Payne, *Cerebral Autoregulation: Control of Blood Flow in the Brain*. 2016.
- [5] R. B. Panerai, “Cerebral autoregulation: From models to clinical applications,” *Cardiovascular*

- Engineering*, vol. 8, no. 1. pp. 42–59, 2008.
- [6] G. Mader, M. Olufsen, and A. Mahdi, “Modeling Cerebral Blood Flow Velocity During Orthostatic Stress,” *Ann. Biomed. Eng.*, vol. 43, no. 8, pp. 1748–58, Aug. 2015.
  - [7] A. A. Birch, “Assessment of Cerebral Autoregulation Using Sinusoidal Lower Body Negative Pressure,” 2005.
  - [8] F. D. Schönbrodt and M. Perugini, “At what sample size do correlations stabilize?,” *J. Res. Pers.*, vol. 47, no. 5, pp. 609–612, 2013.
  - [9] F. P. Tiecks, A. M. Lam, R. Aaslid, and D. W. Newell, “Comparison of Static and Dynamic Cerebral Autoregulation Measurements,” *Stroke*, vol. 26, no. 6, 1995.
  - [10] E. W. Lang, H. M. Mehdorn, N. W. C. Dorsch, and M. Czosnyka, “Continuous monitoring of cerebrovascular autoregulation: a validation study,” *J. Neurol. Neurosurg. Psychiatry*, vol. 72, no. 5, pp. 583–6, May 2002.
  - [11] J. Liu, D. M. Simpson, and R. Allen, “High spontaneous fluctuation in arterial blood pressure improves the assessment of cerebral autoregulation,” *Physiol. Meas.*, vol. 26, no. 5, pp. 725–41, 2005.
  - [12] Y. Liu, A. A. Birch, and R. Allen, “Dynamic cerebral autoregulation assessment using an ARX model: comparative study using step response and phase shift analysis,” *Med. Eng. Phys.*, vol. 25, no. 8, pp. 647–653, 2003.
  - [13] R. B. Panerai, P. J. Eames, and J. F. Potter, “Variability of time-domain indices of dynamic cerebral autoregulation,” *Physiol. Meas.*, vol. 24, no. 2, pp. 367–81, May 2003.
  - [14] S. K. Piechnik, X. Yang, M. Czosnyka, P. Smielewski, S. H. Fletcher, A. L. Jones, and J. D. Pickard, “The continuous assessment of cerebrovascular reactivity: a validation of the method in healthy volunteers,” *Anesth. Analg.*, vol. 89, no. 4, pp. 944–9, Oct. 1999.
  - [15] M. Reinhard, M. Roth, T. Müller, M. Czosnyka, J. Timmer, and A. Hetzel, “Cerebral autoregulation in carotid artery occlusive disease assessed from spontaneous blood pressure fluctuations by the correlation coefficient index,” *Stroke*, vol. 34, no. 9, pp. 2138–44, Sep. 2003.
  - [16] A. Mahdi, D. Nikolic, A. A. Birch, M. S. Olufsen, D. M. Simpson, R. Panerai, and S. J. Payne, “Increased blood pressure variability upon standing up improves reproducibility of cerebral autoregulation indices,” *arXiv:1705.04942*, 2017.
  - [17] F. A. Sorond, J. M. Serrador, R. N. Jones, M. L. Shaffer, and L. A. Lipsitz, “The Sit-to-Stand Technique for the Measurement of Dynamic Cerebral Autoregulation,” *Ultrasound Med. Biol.*, vol. 35, no. 1, pp. 21–29, 2009.
  - [18] N. Angarita-Jaimes, H. Kouchakpour, J. Liu, R. B. Panerai, and D. M. Simpson, “Optimising the assessment of cerebral autoregulation from black box models,” *Med. Eng. Phys.*, vol. 36, no. 5, pp. 607–612, 2014.
  - [19] P. J. Eames, M. J. Blake, R. B. Panerai, and J. F. Potter, “Cerebral autoregulation indices are unimpaired by hypertension in middle aged and older people,” *Am. J. Hypertens.*, vol. 16, no. 9 I, pp. 746–753, 2003.
  - [20] B. M. Deegan, J. M. Serrador, K. Nakagawa, E. Jones, F. A. Sorond, and G. O’laighin, “The effect of blood pressure calibrations and transcranial Doppler signal loss on transfer function estimates of cerebral autoregulation,” *Med. Eng. Phys.*, vol. 33, no. 5, pp. 553–62, Jun. 2011.
  - [21] A. S. S. Meel-van den Abeelen, D. L. K. de Jong, J. Lagro, R. B. Panerai, and J. A. H. R. Claassen, “How measurement artifacts affect cerebral autoregulation outcomes: A technical note on transfer function analysis,” *Med. Eng. Phys.*, vol. 38, no. 5, pp. 490–7, May 2016.
  - [22] A. Mahdi, E. Rutter, and S. J. Payne, “Effects of non-physiological blood pressure artefacts on measures of cerebral autoregulation,” *arXiv:1612.09486*, 2017.
  - [23] R. K. Pearson, “Outliers in process modeling and identification,” *IEEE Trans. Control Syst.*

*Technol.*, vol. 10, no. 1, pp. 55–63, 2002.

- [24] D. Nikolic, E. Katsogridakis, R. B. Panerai, and D. M. Simpson, “Tracking time-varying changes in the cerebral autoregulation measures,” in *6th International Meeting on Cerebral Haemodynamic Regulation*, 2016.

## 5 Appendix

### 5.1 An implementation details of ARI

The implementation of ARI used here follows Tiecks et al. [9]. We denote the beat-to-beat average of ABP and CBFV by  $P[k]$  and  $V[k]$ , respectively; the mean values of  $P[k]$  and  $V[k]$  by  $\bar{P}$  and  $\bar{V}$ . The input  $P[k]$  is normalized

$$dP[k] = \frac{P[k] - \bar{P}}{\bar{P} - P_{cr}} \quad (\text{A.1})$$

where  $P_{cr} = 12$  mmHg is the critical closing pressure [52]. We estimate  $V[k]$  using the following difference model

$$\begin{aligned} x_1[k] &= x_1[k-1] + \frac{dP[k] - x_2[k-1]}{fT} \\ x_2[k] &= x_2[k-1] + \frac{x_1[k-1] - 2Dx_2[k-1]}{fT} \\ \hat{V}[k] &= \bar{V}(1 + dP[k] - Kx_2[k]) \end{aligned} \quad (\text{A.2})$$

where  $f$ ,  $D$ ,  $T$  and  $K$  are the sampling frequency, damping factor and time constant parameters, respectively. The combinations of ten different values of  $(T, D, K)$  (see [9]) are used to generate ten models  $\hat{V}_j[k]$ , corresponding to different grades of autoregulation ( $j = 0, \dots, 9$ ). The difference between the predicted and measured CBFV is computed as  $d_j = \|\bar{V}_j[k] - V[k]\| / \bar{V}$ , where  $\|\cdot\|$  is the  $\ell^2$ -norm. By  $f_{ARI}(s)$  we denote the interpolation by cubic splines of the values  $d_j$ . Finally, the ARI is determined by calculating the  $s$  that minimizes  $f_{ARI}(s)$ , that is:

$$ARI = \arg \min f_{ARI}(s), \quad s \in \{0, \dots, 9\}. \quad (\text{A.3})$$

## 6 Plots and Tables

	ABP	CBFV-L	etCO <sub>2</sub>	HR
	[mmHg]	[cm/s]	[mmHg]	[beats/min]
Mean	74.74	72.79	36.56	69.38
SD	7.91	6.99	3.84	9.18
CoV	0.11	0.10	0.10	0.13

Table 1. **Data characteristics.** The mean, standard deviation (SD) and the coefficient of variation (CoV) for the signals considered in this study.

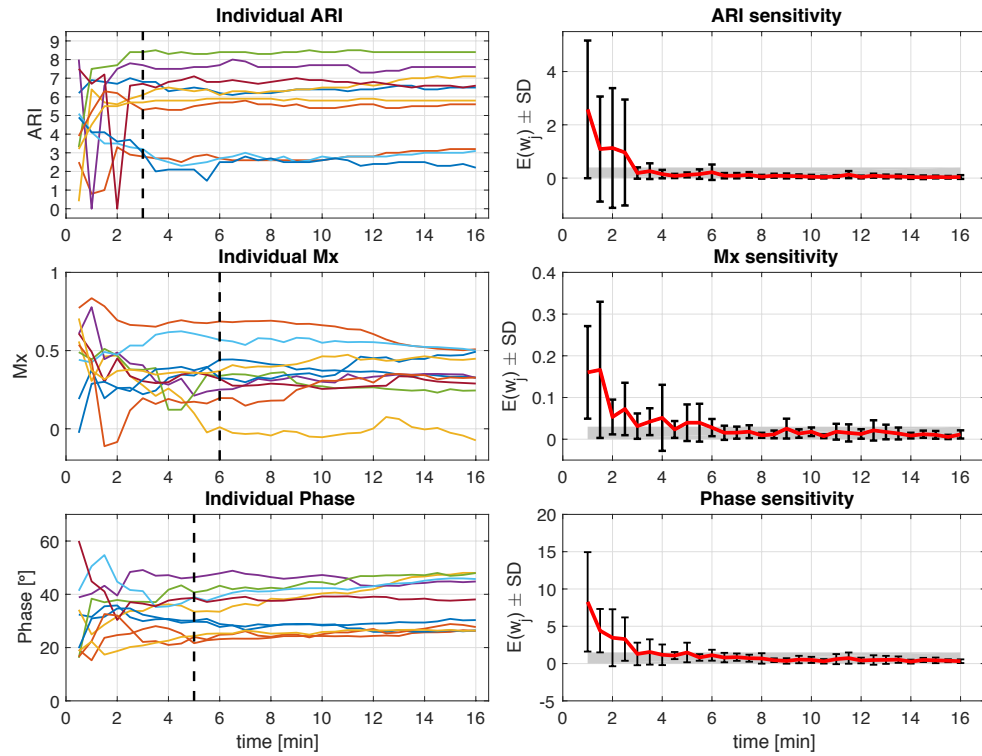


Figure 1 **Expanding window sensitivity.** *Left:* The trajectories of ARI (top row), Mx (middle row) and Phase (bottom row) calculated for the 30-second increments of the expanding window. *Right:* The mean expanding window sensitivity for ARI (top row), Mx (middle row) and Phase (bottom row). The graphs show the mean (red line) and standard deviation (vertical bars) of the expanding window sensitivity,  $E(w_j) \pm SD$ , calculated across all subjects. The vertical dotted lines in the left column show the point of stability corresponding to the selected corridor of stability (grey area in the right column), see Section 2.5.



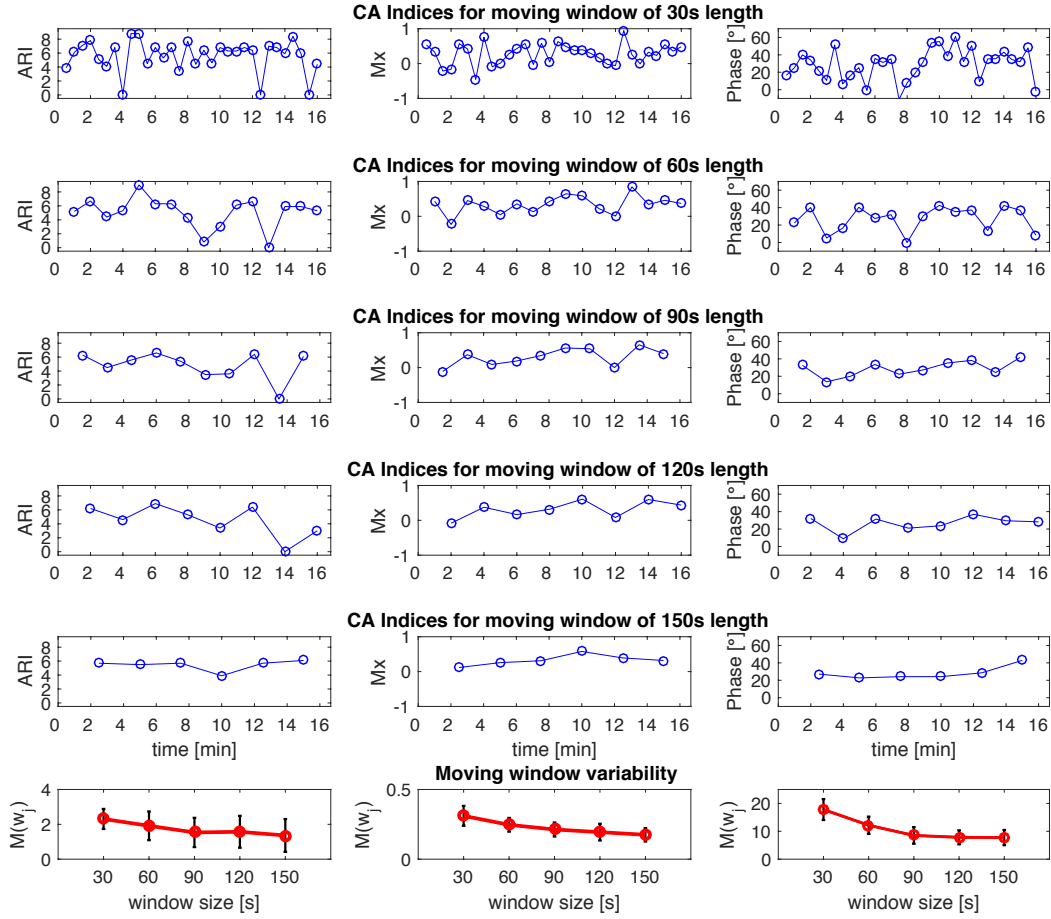


Figure 2: **Moving window variability.** Top five rows show (blue line) an example of ARI (left column), Mx (middle column) and Phase (right column) computed for the moving windows of size 30, 60, 90, 120 and 150s for one subject. Bottom row (red line) show the mean of standard deviations of CA measures computed along the recording (as shown above) for each window size averaged over all subjects.